Particle Radiation at Earth and Through the Inner Solar System

P. Quinn, C. Joyce, R. Winslow, J. Chen, F. Rahmanifard, N. A. Schwadron, K. Kozarev, N. Lugaz, J. Linker, M. Gorby, Pete Riley, Z. Mikic, R. Lionello, T. Torok, V. Titov, B. Chandran, J. Cooper, M. Desai, K. Germaschewki, J. Giacalone, P. Isenberg, J. Kasper, K. Korreck, M. Lee, P. MacNeice, H. Spence, S. Smith, M. Stevens

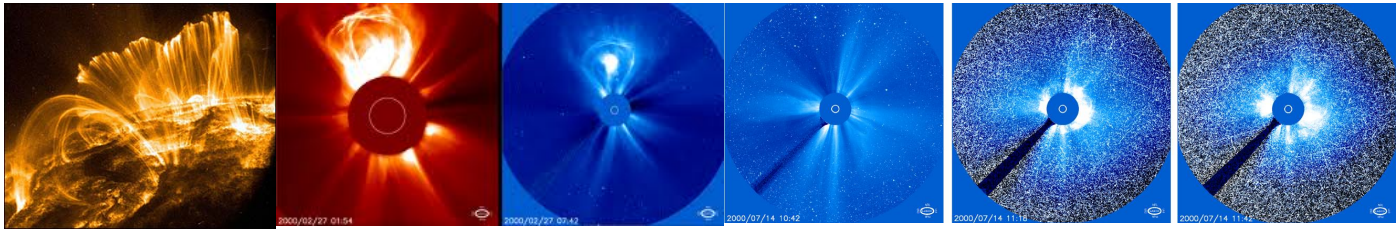

- Highest GCR doses in space age in recent cycle 23 solar minima
- Continues trend observed by Ulysses, ACE

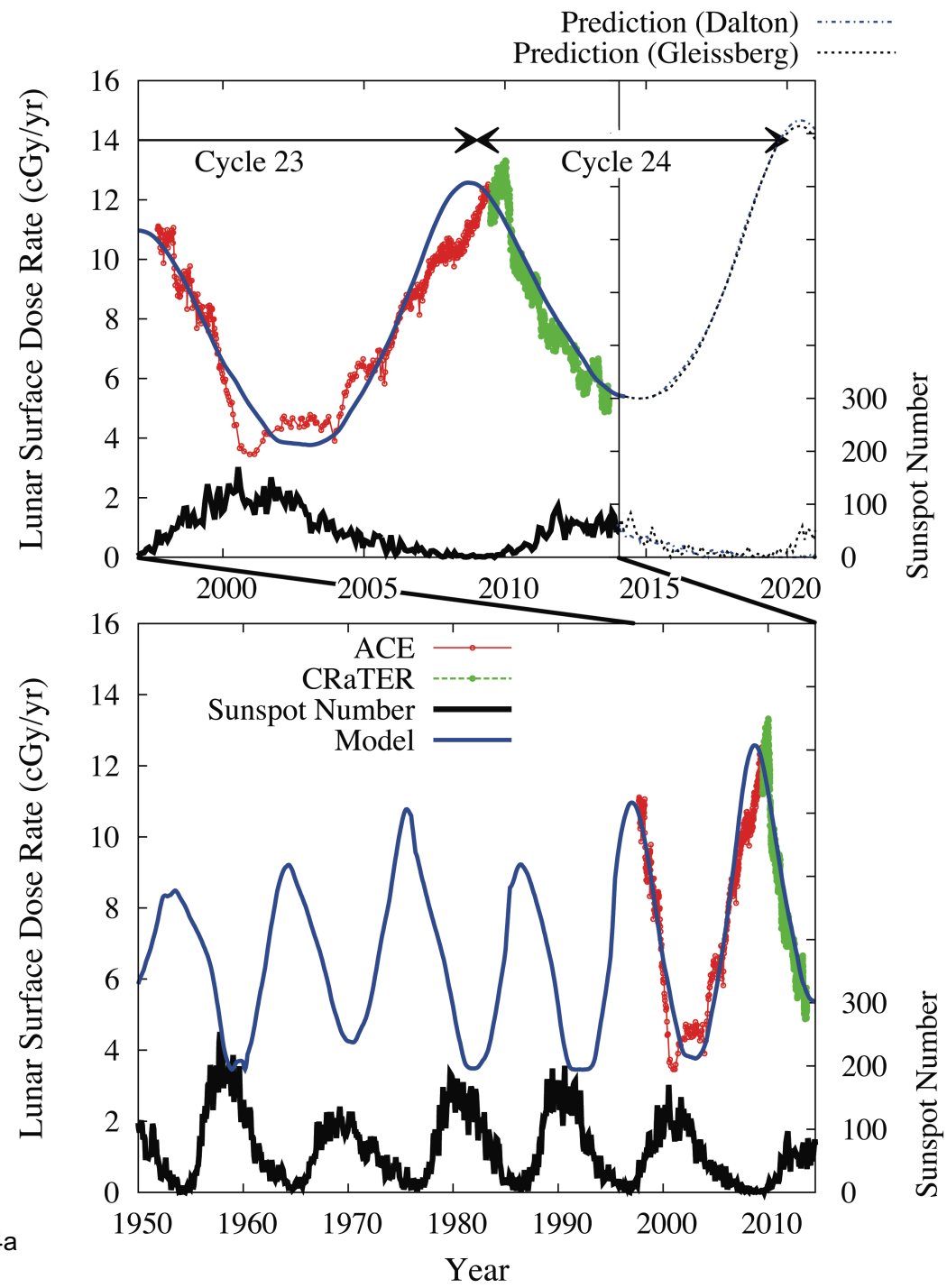

SCHWADRON ET AL., SPACE WEATHER, 2014a

Implications of the Changing Space Weather Environment

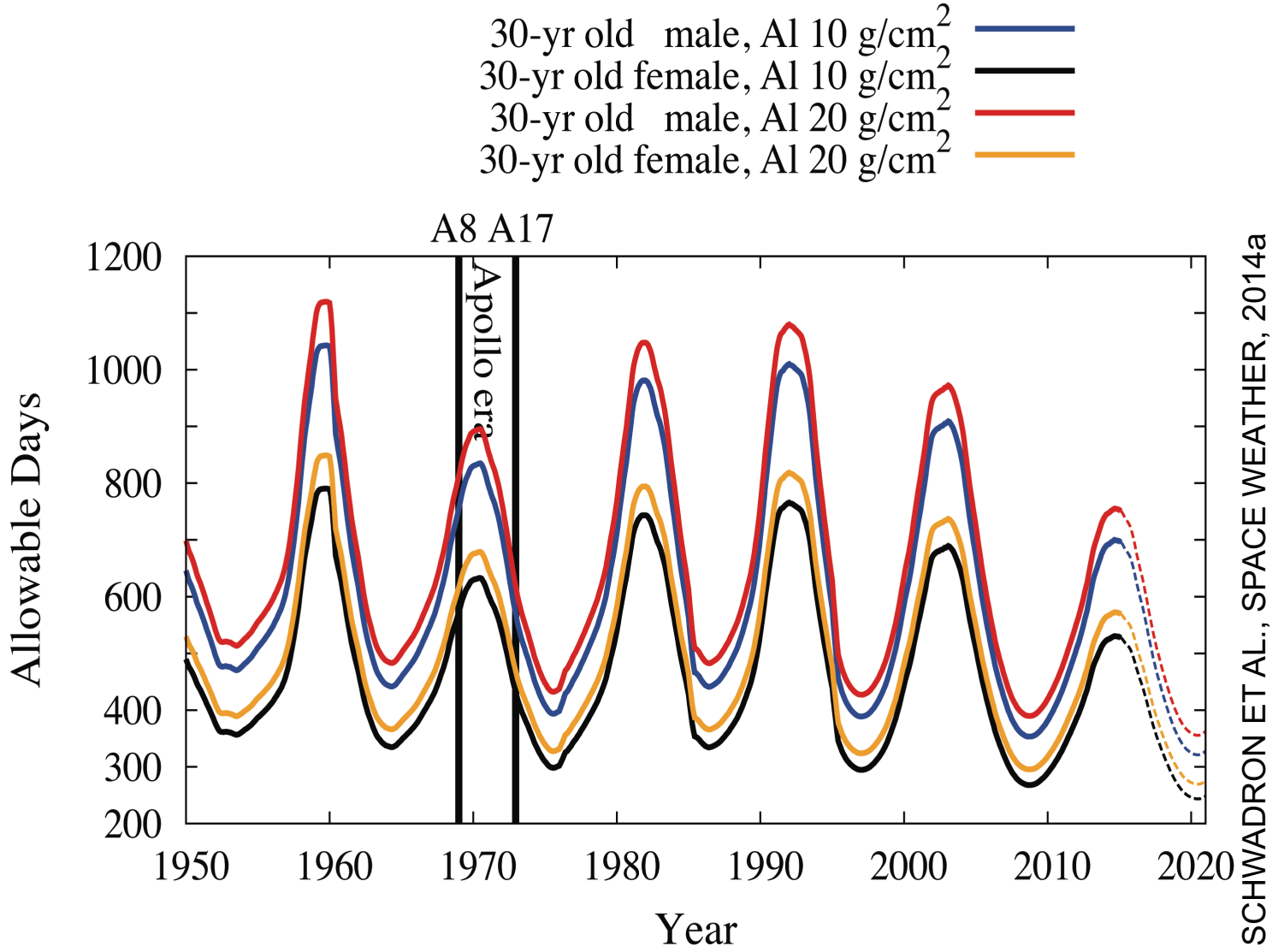

Strong Reduction in Field Possible – Much Higher GCR Flux

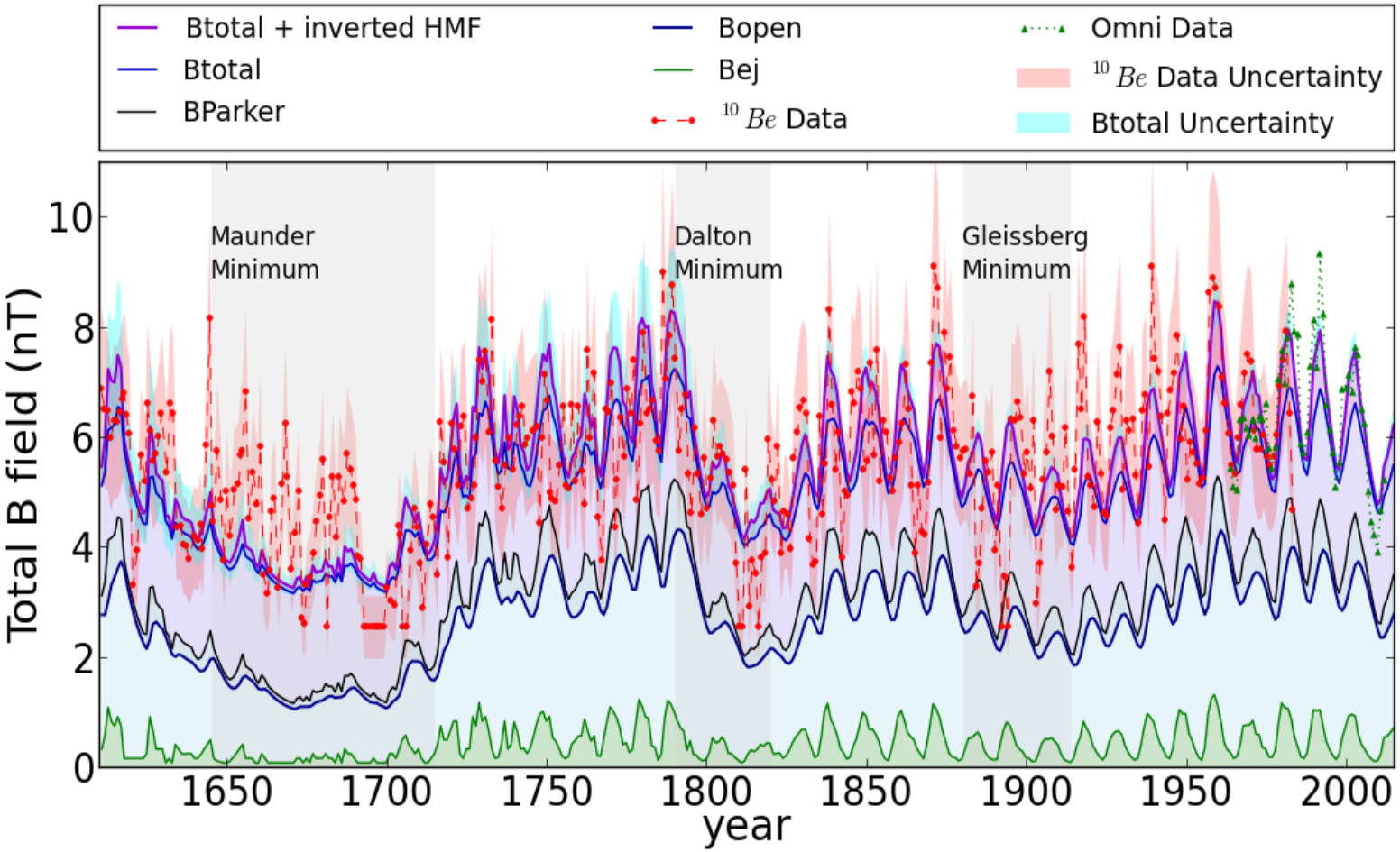

Rahmanifard et al., 2016

Radiation Through Earth's Atmosphere

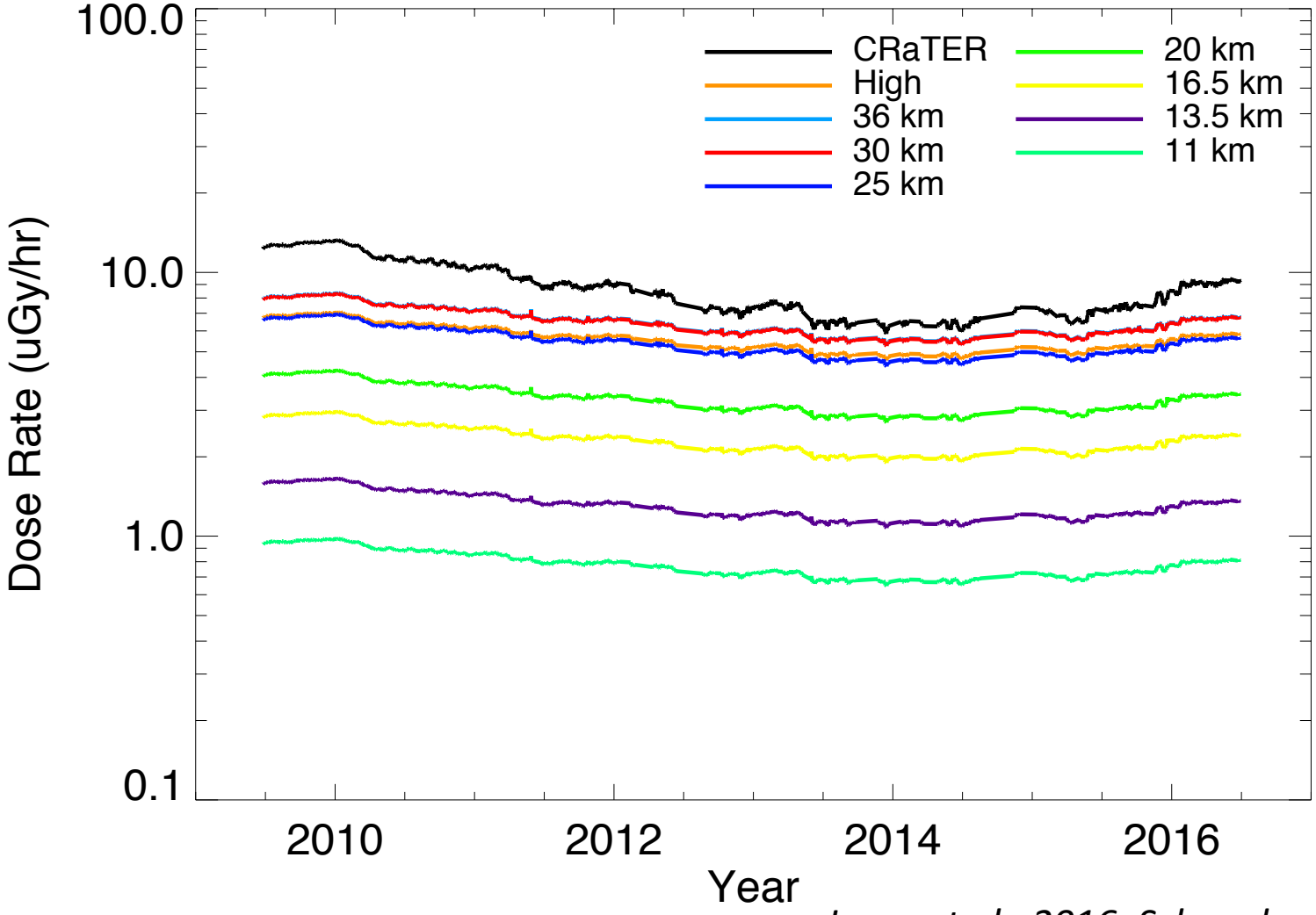

Joyce et al., 2016, Schwadron et al., 2017

Radiation at Aviation Altitudes

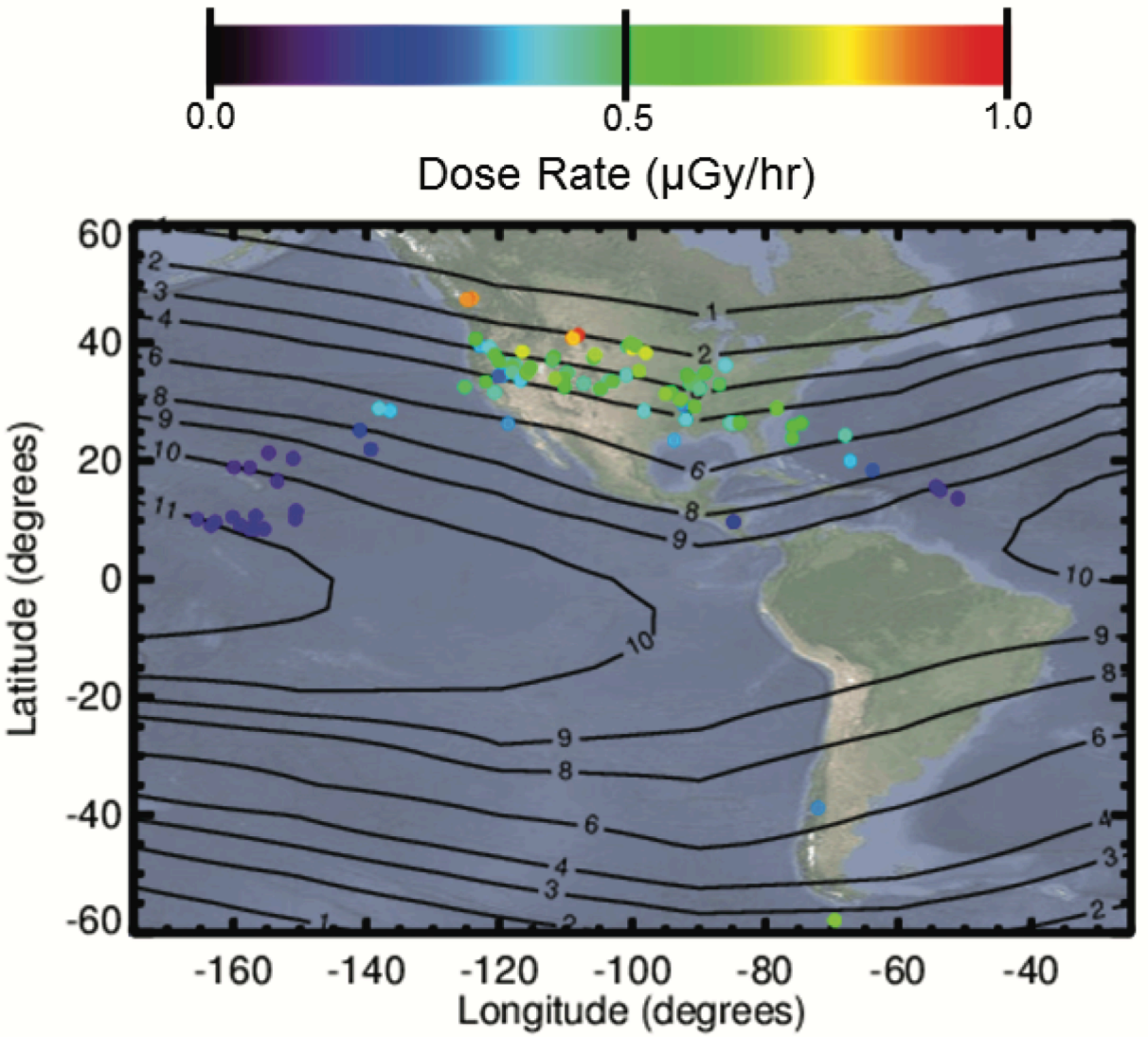

Joyce et al., 2016, Schwadron et al., 2017

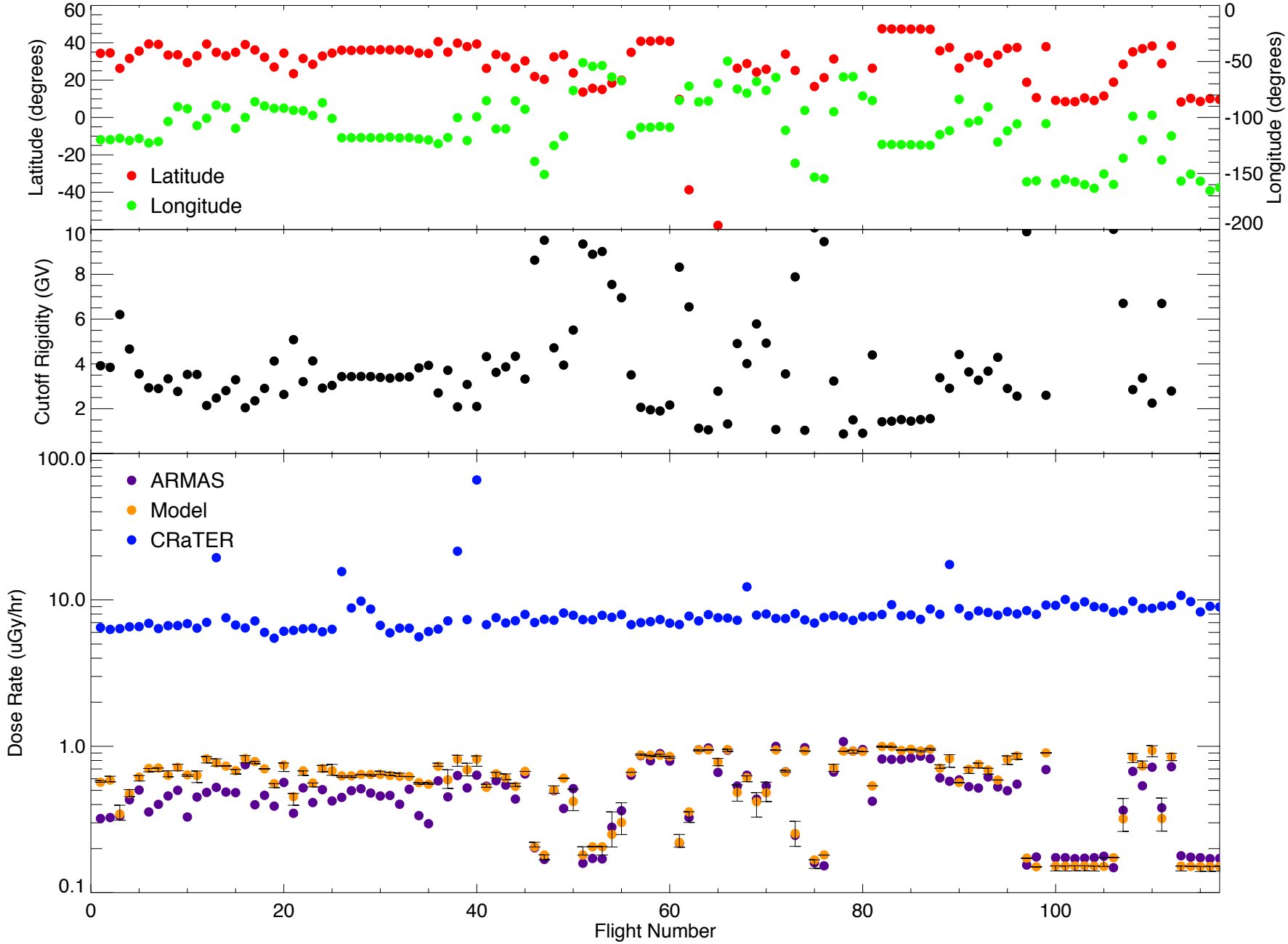

Joyce et al., 2016, Schwadron et al., 2017

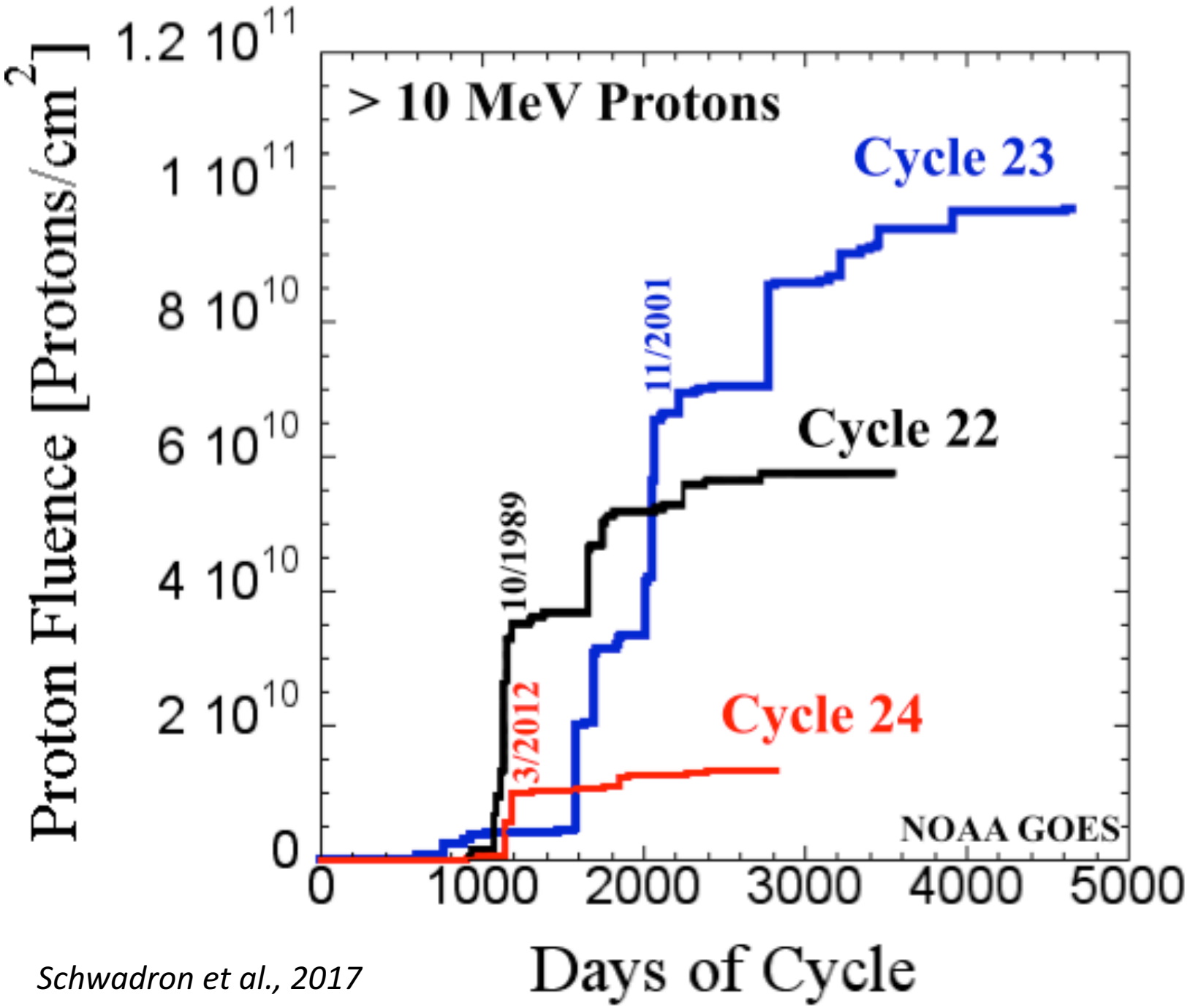

Schwadron et al., 2017

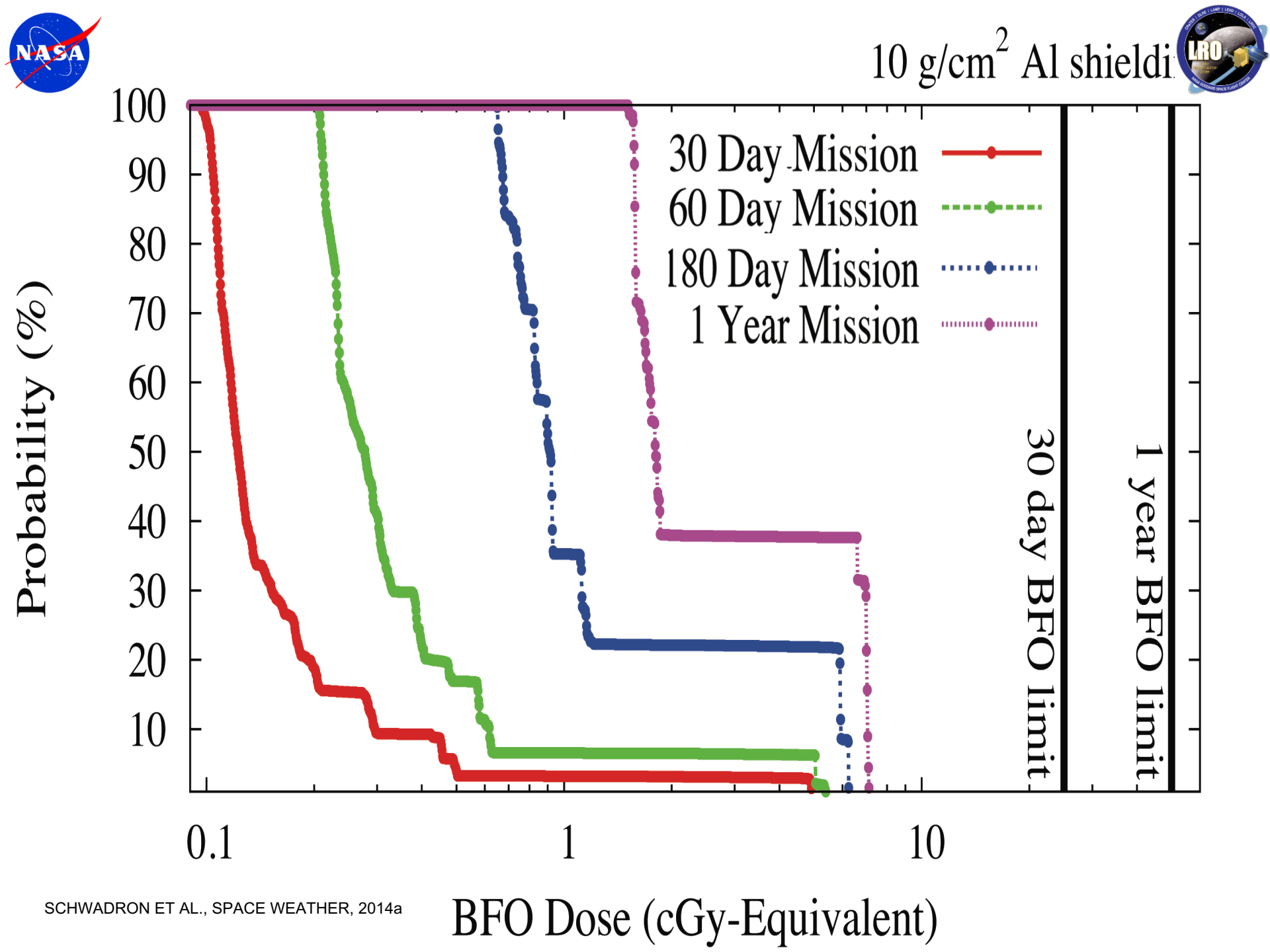

SCHWADRON ET AL., SPACE WEATHER, 2014a

Characterizing the Earth-Moon-Mars SEP Radiation Environment

January, March, and May 2012 SEP events.

Dose rates measured by CRaTER at the Moon, MSL/RAD during cruise to Mars, and predicted by PREDICCS.

PREDICCS takes SEP measurements and uses EPREM to simulate the transport to Earth and Mars.

Converts proton flux to dose rate behind various levels of shielding.

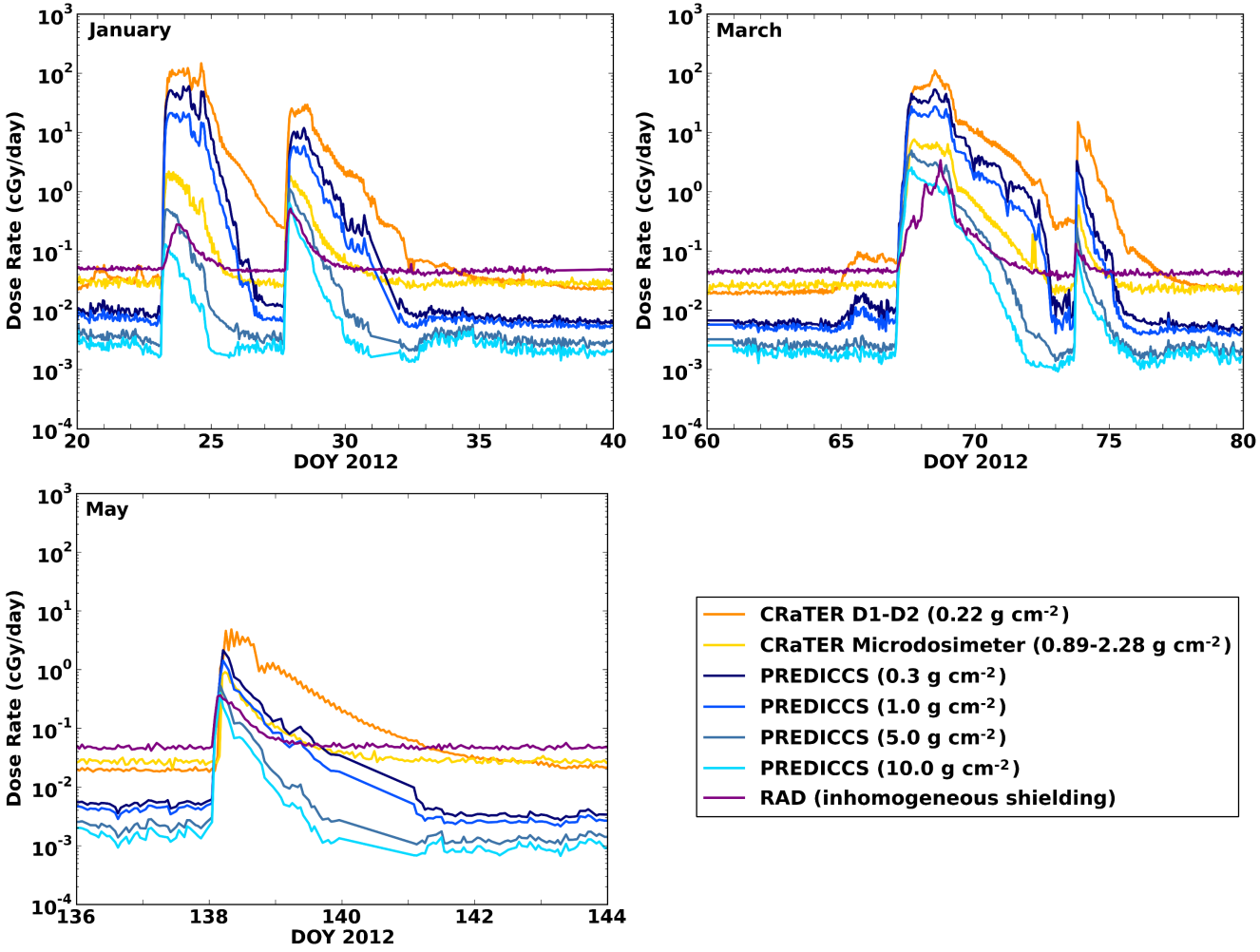

Quinn et al. 2017 (under review)

Characterizing the Earth-Moon-Mars SEP Radiation Environment

Dose accumulated during January, March, and May 2012 SEP events at location of MSL (except CRaTER).

GCR background removed.

Dose accumulated behind 0.3 g/cm^2 shielding exceeds the 30-day skin limit for the January and March events.

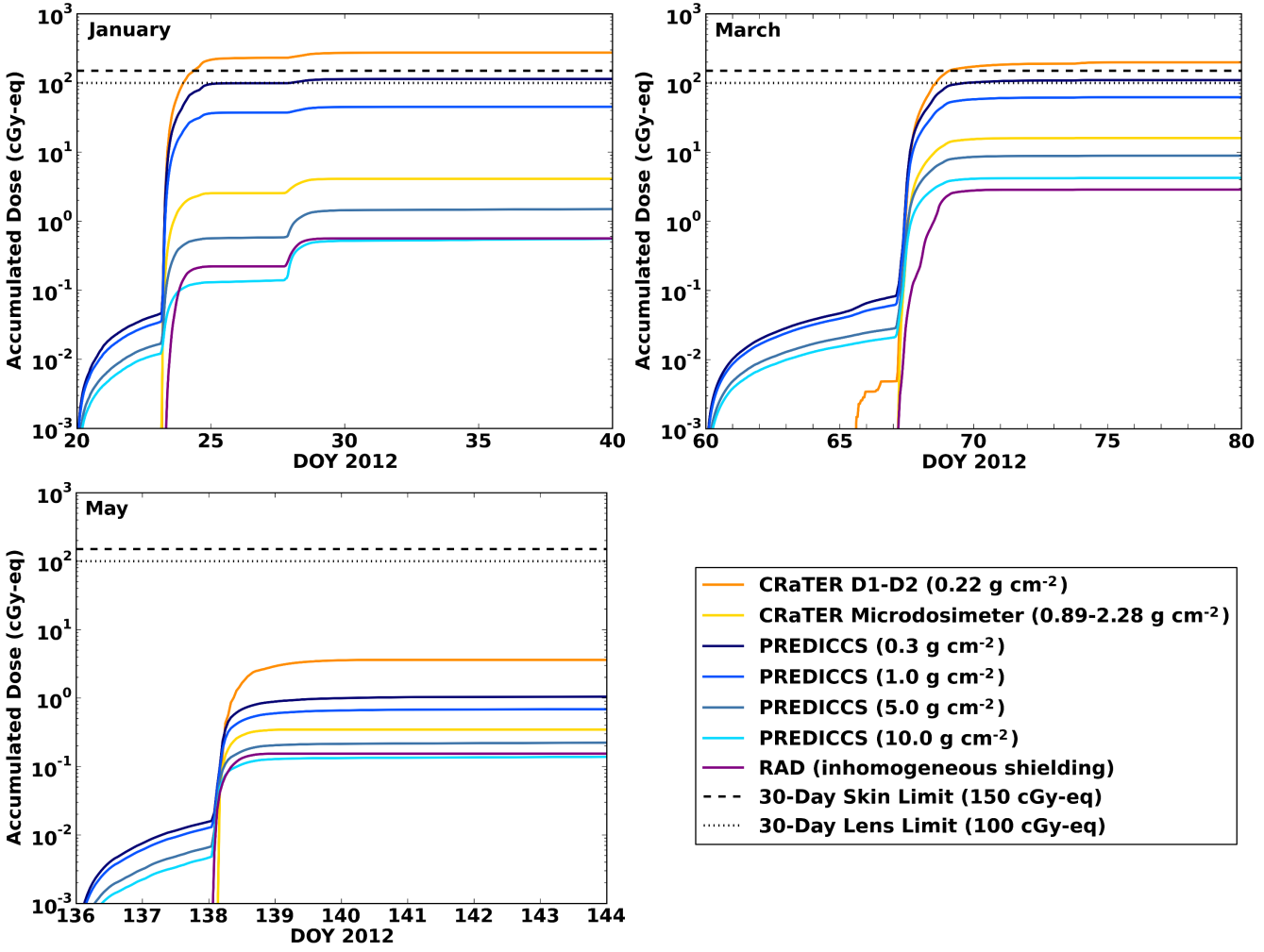

Quinn et al. 2017 (under review)

Characterizing the Earth-Moon-Mars SEP Radiation Environment

Accumulated dose during each SEP event as a function of aluminum-equivalent shielding.

RAD had an average shielding of about 16 g/cm^2.

Percent differences between PREDICCS and RAD range from as little as 2% to 54%.

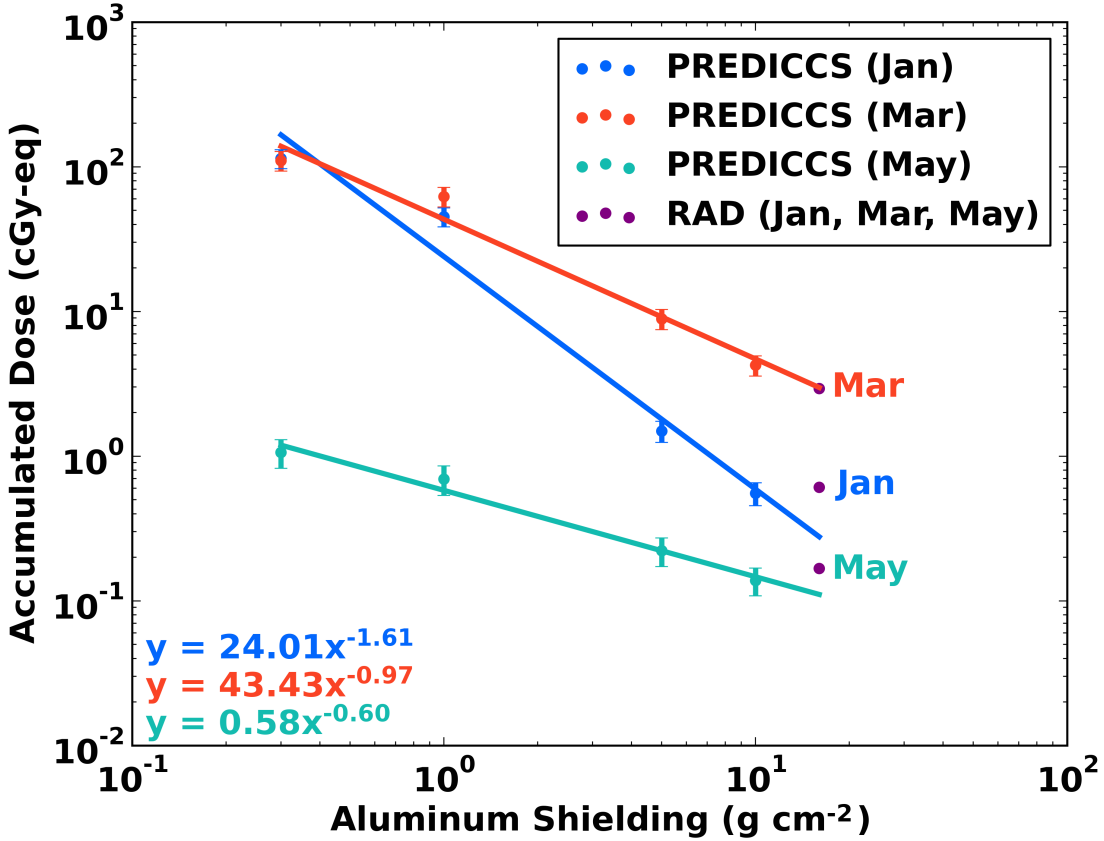

Quinn et al. 2017 (under review)

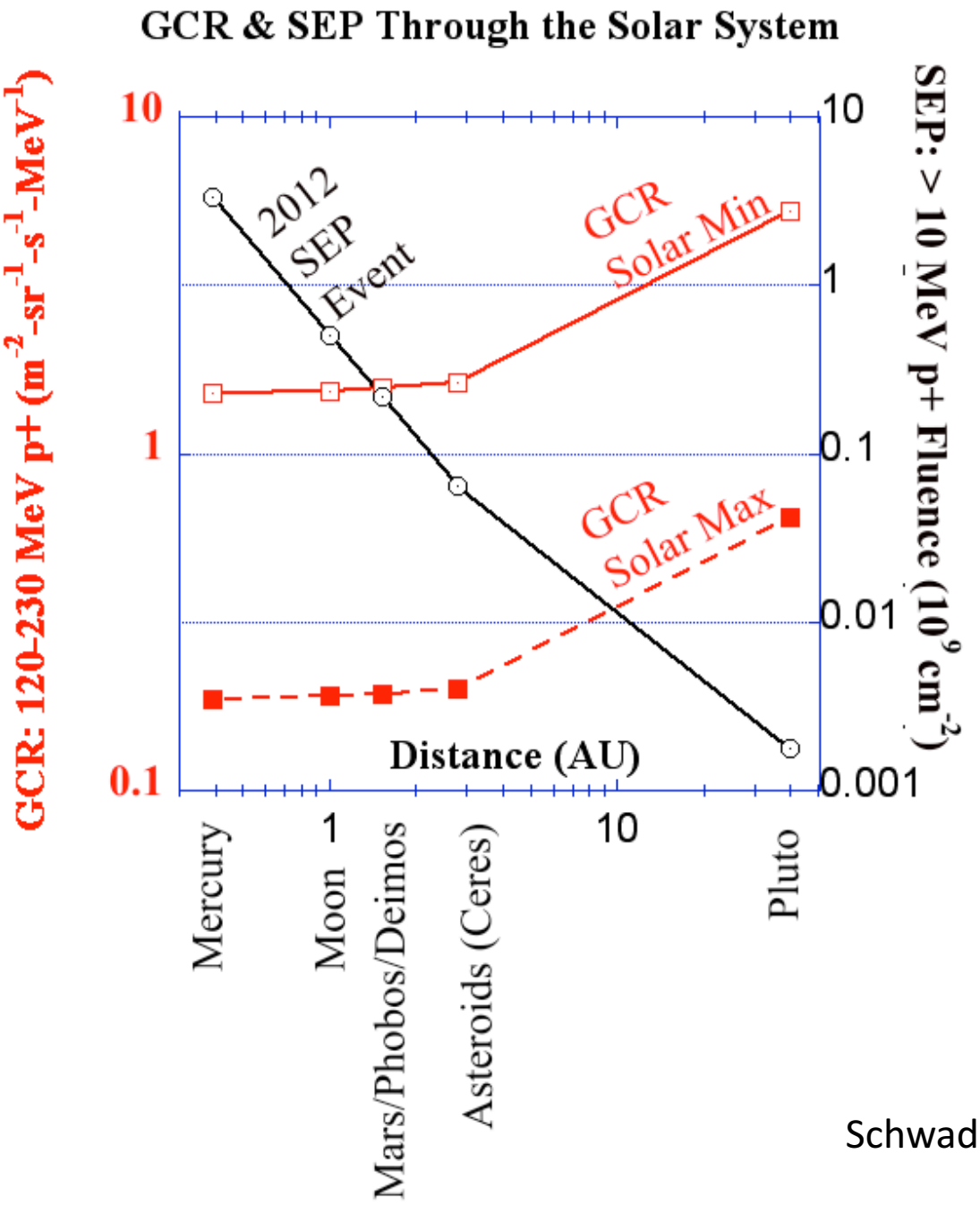

Schwadron et al., 2017

Deriving the Scattering Mean Free Path of Helium Pickup Ions

Pickup ion measurements derive a longitudinal inflow direction of the interstellar wind that is consistently higher than neutral measurements.

Simulating the transport between neutral focusing cone and pickup focusing cone allows us to derive parameters.

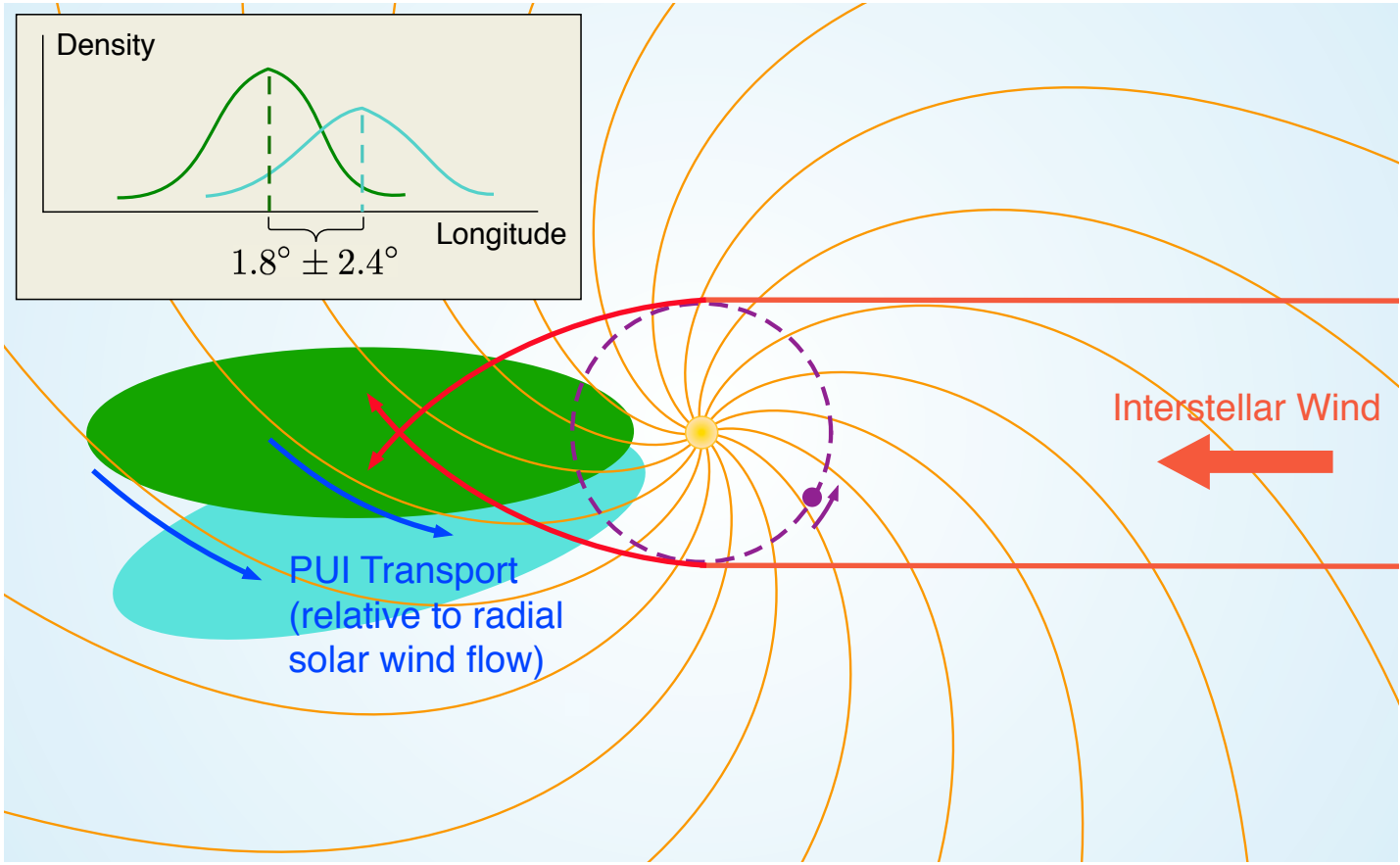

Quinn et al. 2016

The transport of helium pickup ions is simulated using EPREM for a mean free path range of 0.1 AU to 1 AU.

The longer the mean free path, the more the pickup focusing cone shifts compared to the neutral focusing cone.

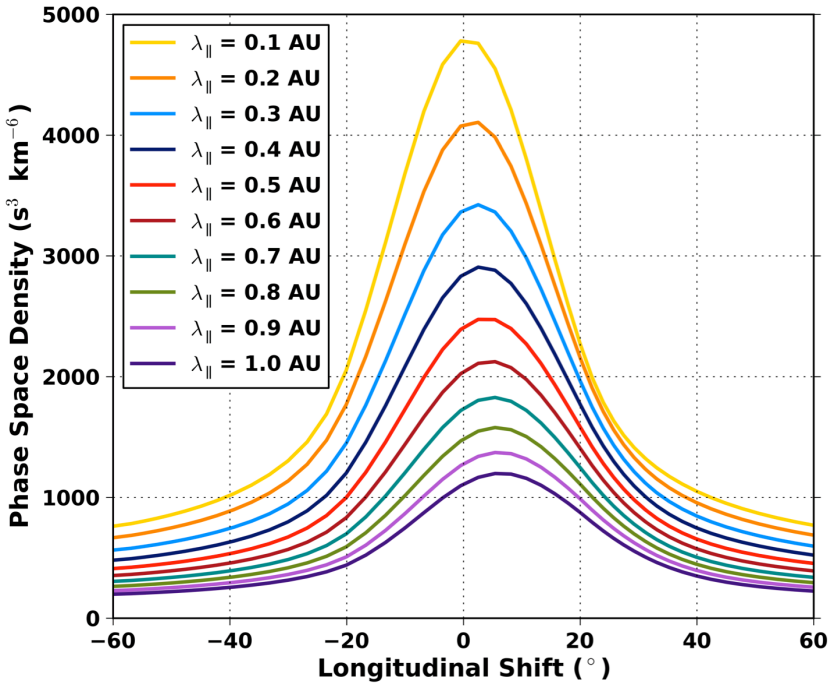

The peak longitudes are plotted against mean free path.

The modeled shift intersects the observed shift at 0.19 AU +0.29(-0.19) AU.

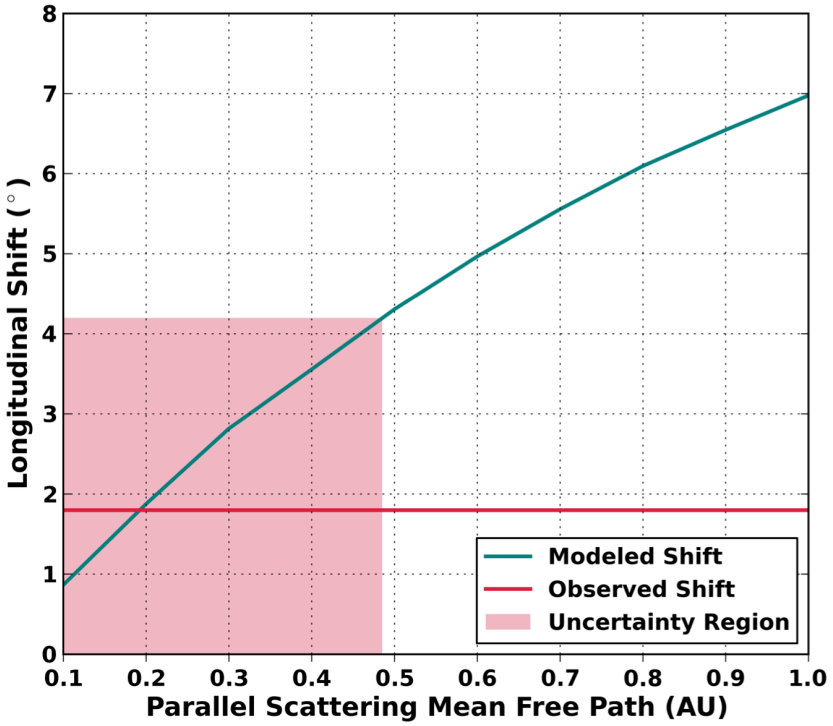

The amount of shift is suggested to be due to an anisotropic velocity distribution.

By calculating the average azimuthal velocity of the pickup ions, we see that the pickup ion distribution reaches ~8% of the solar wind speed inside 1 AU.

Although this velocity is small, it's enough to shift the focusing cone by the 1.8 degree observation difference.

Using EPREM's ability to turn transport effects on or off, EPREM is ran for the 4 cases shown in the figure caption.

The amount of shift from each transport effect is found by differencing the peak longitude with the previous case.

Pitch-angle scattering	20.00%
Adiabatic focusing	69.43%
Perpendicular diffusion	10.56%
Particle drift	<0.01%

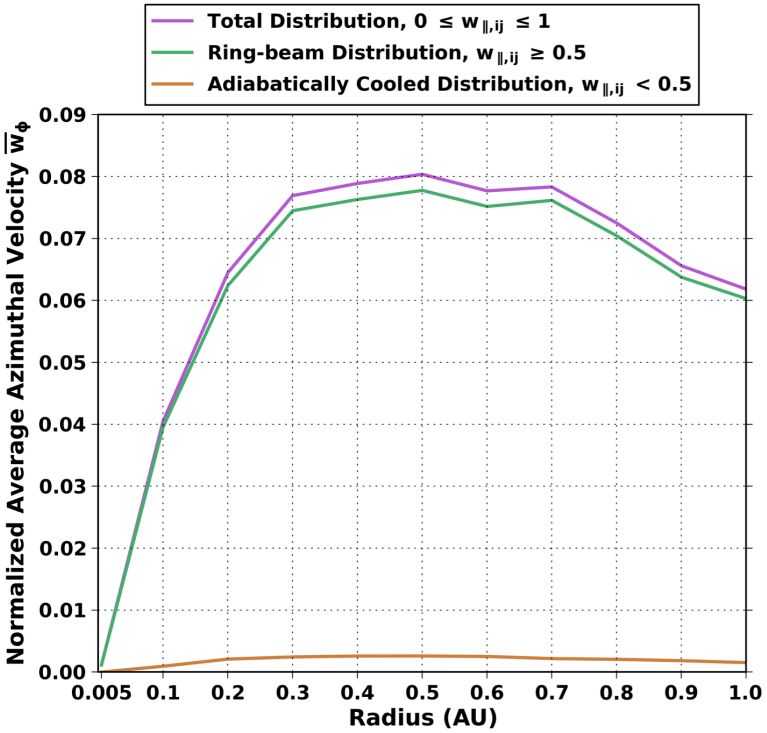

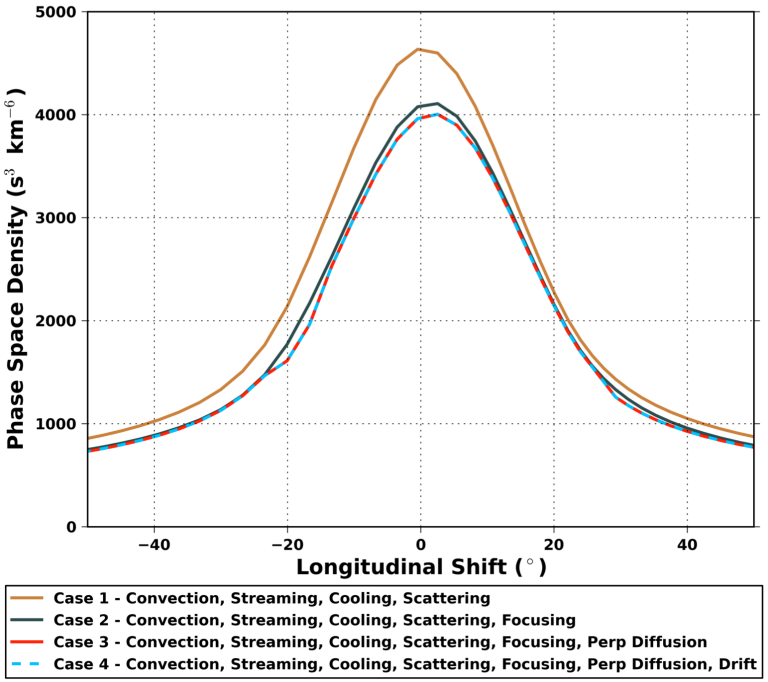

Pickup Ion acceleration in a CIR

Coupled EPREM with an MHD model (Giacalone et al. 2002) for CIR structures where the forward and reverse shocks have not yet formed.

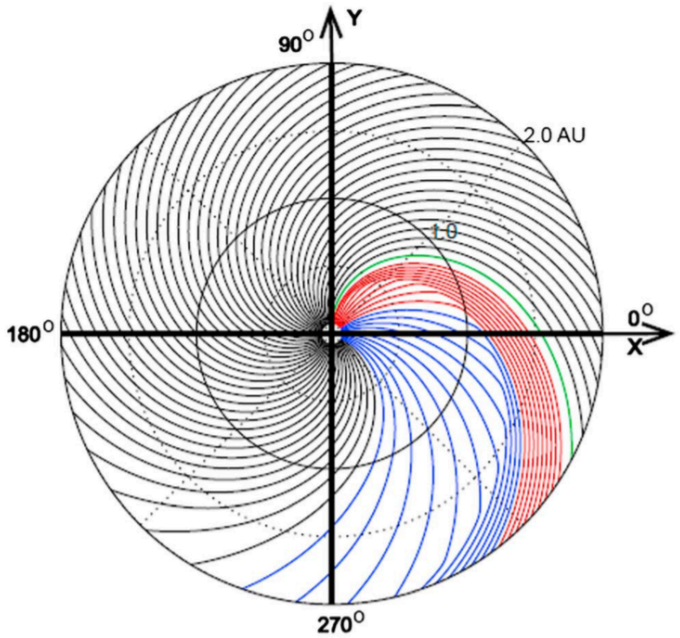

The pickup ion velocity modeled by EPREM within the compression region has a high-energy tail with -5 power law index.

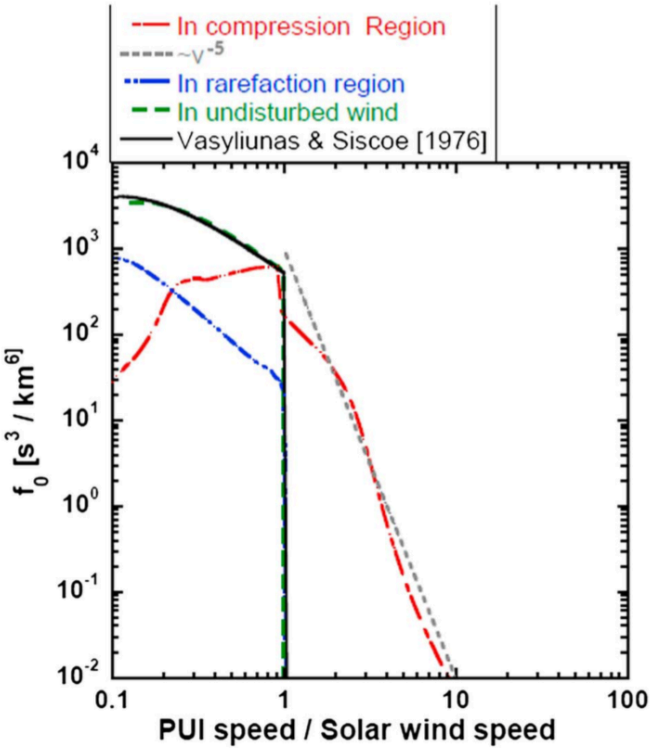

Chen et al. 2015, 2016

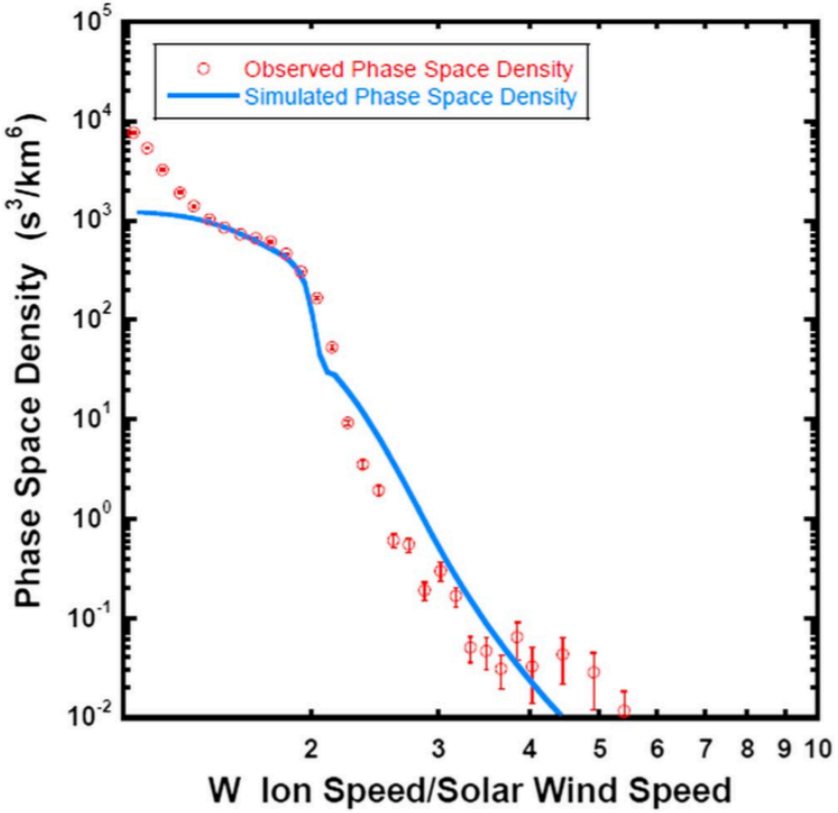

Comparison between modeled velocity distribution and observations from STEREO/PLASTIC.

The tail is sensitive to the velocity gradient associated with the CIR formation causing the power law index to range from -3 to above -10.

This also suggests that the velocity gradient can efficiently create a seed population of pickup ions before a shock forms and without stochastic acceleration.

Chen et al. 2015, 2016

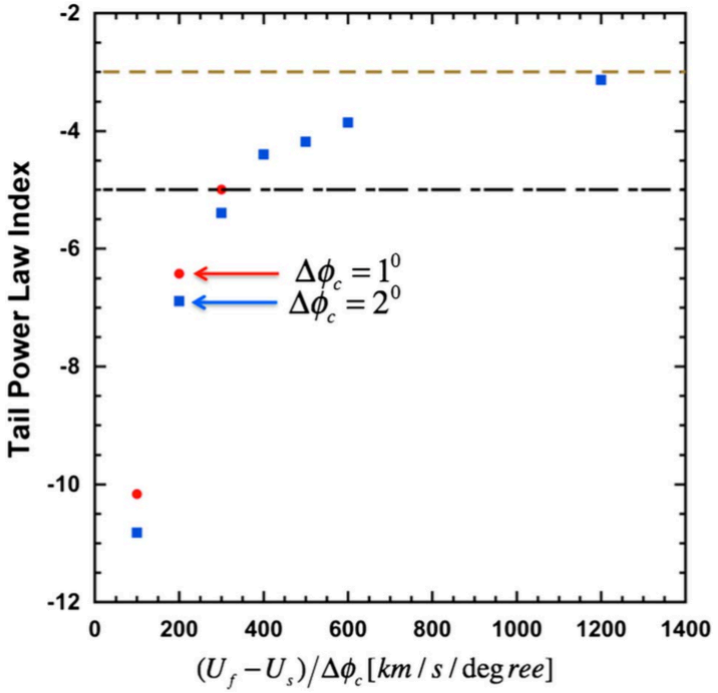

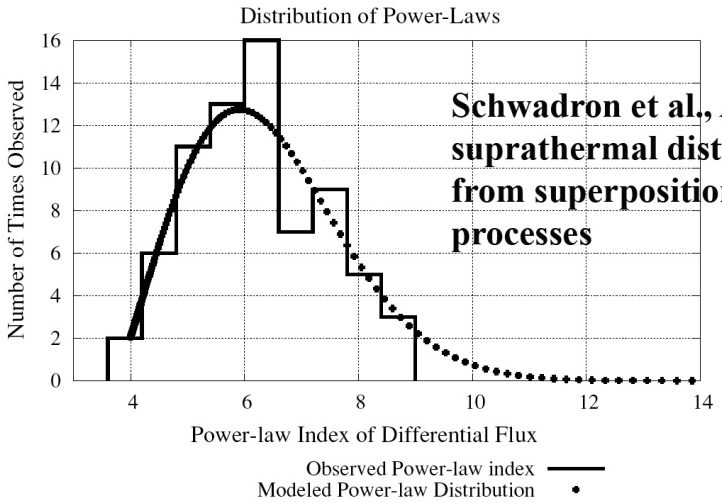

Schwadron et al., ApJ, 2010, suprathermal distributions from superposition of stochastic processes

Matthaeus et al., Phil. Trans, 2015, Intermittency, nonlinear dynamics

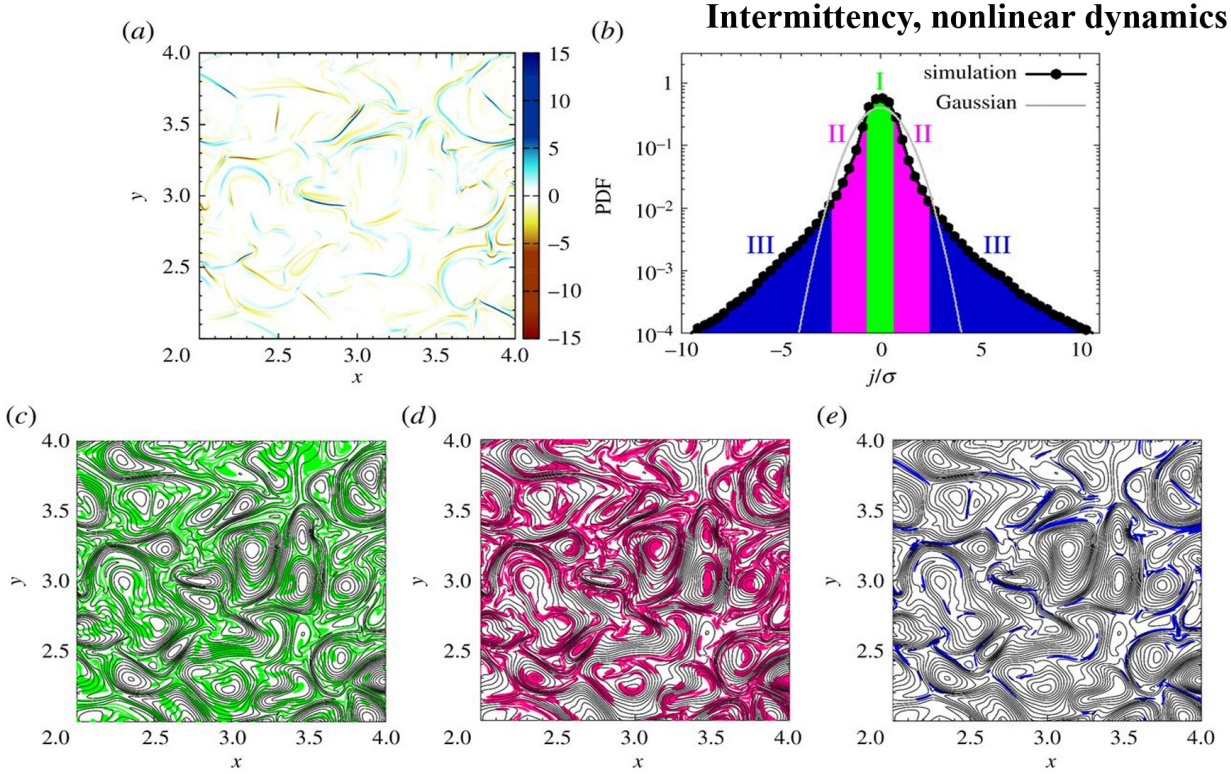

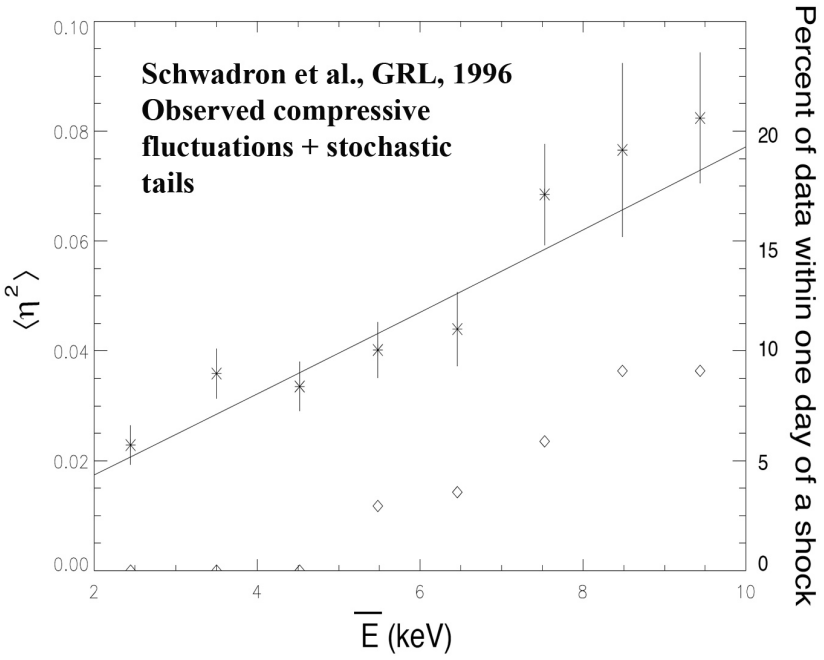

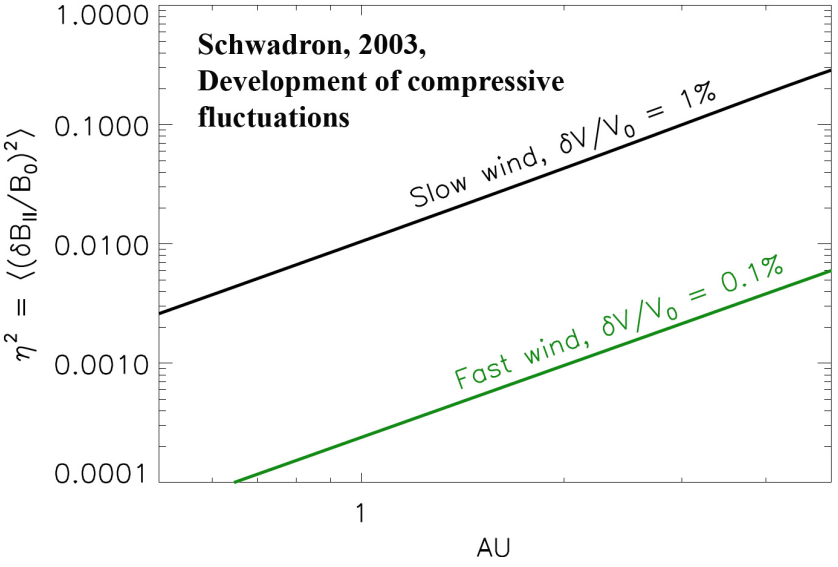

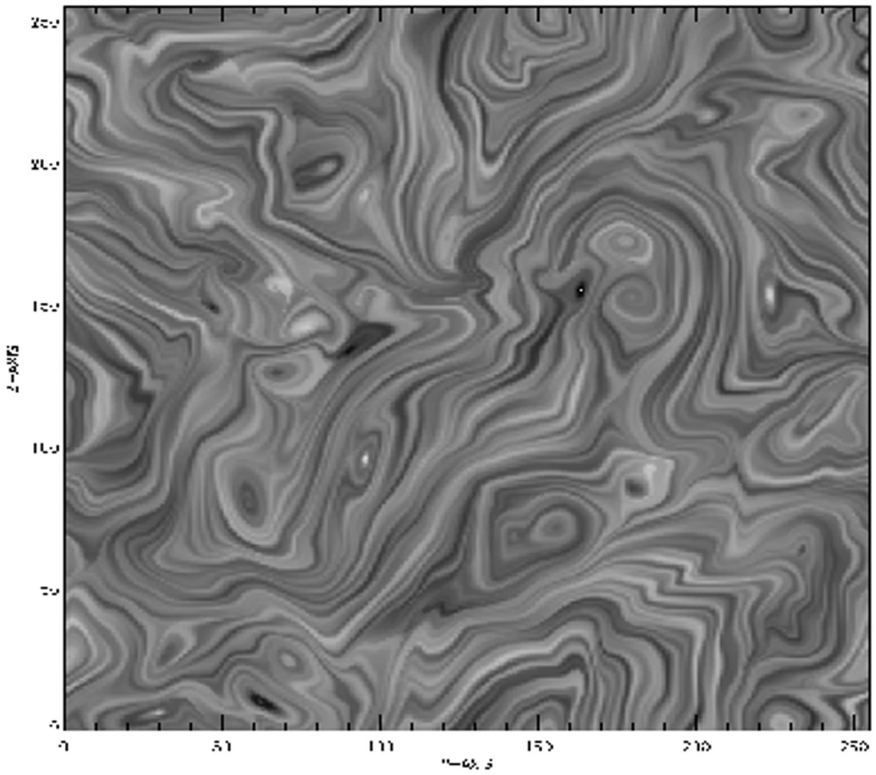

Turbulence and development of in situ compressive field fluctuations

Probing the Production Mechanism of Inner Source Pickup Ions

Inner source pickup ions are produced by the interaction between the solar wind and dust grains orbiting the sun.

Possible production mechanisms include:

- Solar wind neutralization
- **Solar wind recycling**
- Sputtering
- Dust-dust collisions
- Sun-grazing comets

Solar wind recycling – Solar wind ions impact dust grains, are neutralized within the grain, diffuse to the surface, desorb from the grain, then get ionized and picked up by the solar wind.

Quinn et al., 2017 (manuscript under preparation)

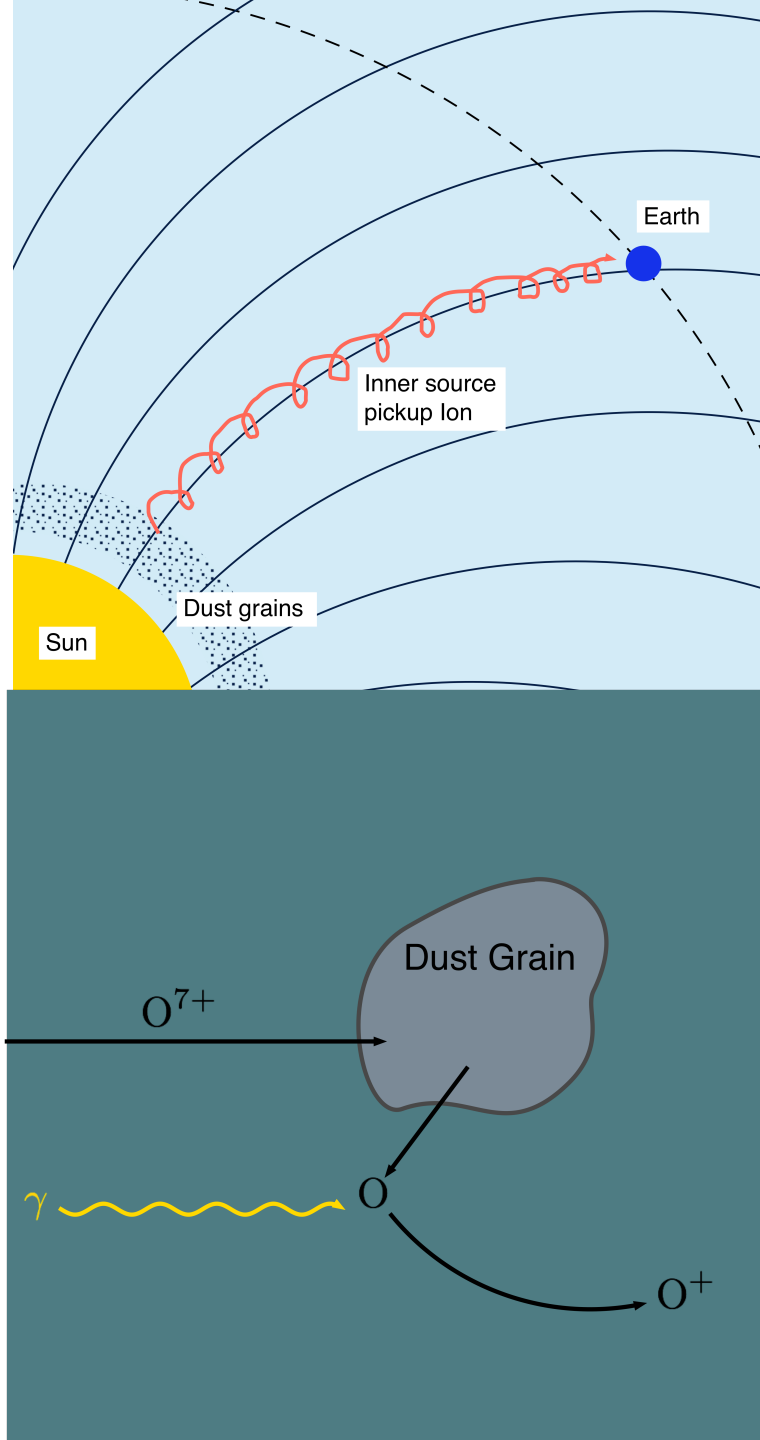

Probing the Production Mechanism of Inner Source Pickup Ions

We use EPREM to simulate the production of inner source pickup ions from solar wind recycling.

The figures show a top-down view of the heliosphere from the sun at the center and out to 5.5 AU. The interstellar wind flows from right to left. Shown is the C+/O+ ratio for low energies (inner source, top figure) and higher energies (interstellar, bottom figure).

The C+/O+ ratio for inner source pickup ions resembles that of the solar wind with more Oxygen than Carbon. However, pickup ion measurements show more Carbon than Oxygen. This shows there must be another production mechanism other than solar wind recycling.

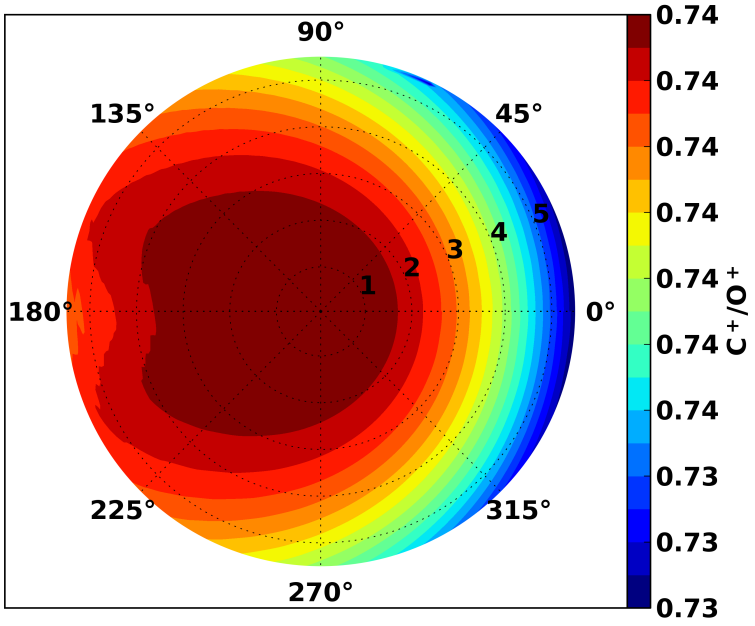

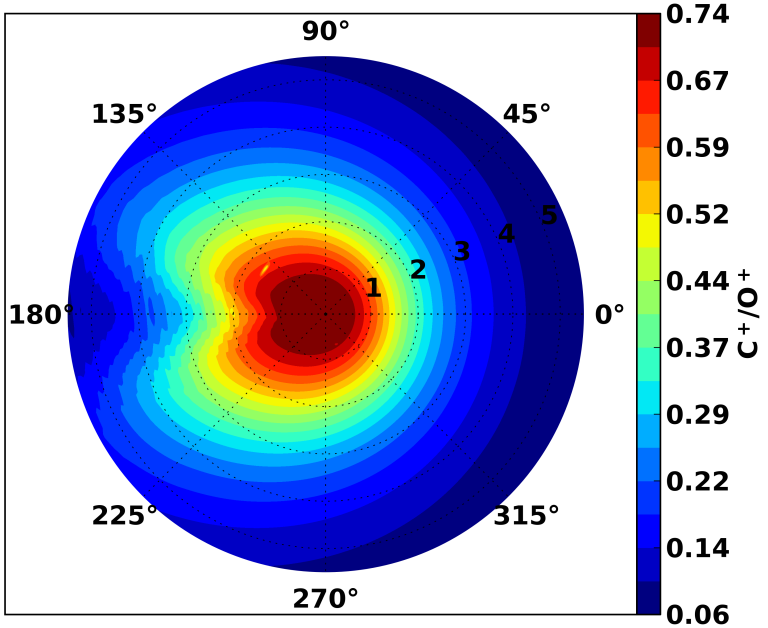

ICME/GCR studies using MESSENGER data

MESSENGER – First spacecraft since 1980's at < 0.5 AU.

- In orbit around Mercury from March 2011 to April 2015.

Areas of study for which MESSENGER data is of high importance:

- Database and characteristics of ICMEs at ~0.3 AU (Winslow et al., 2015)

If used in conjunction with data from other spacecraft:

- ICME evolution in the inner heliosphere (Winslow et al., 2016)
- GCR modulation by ICMEs in the inner heliosphere (Winslow et al. 2017, *in prep.*)
- Validation of ICME propagation models

=> Lay the groundwork for improved geomagnetic storm prediction at Earth using in situ data from < 0.5 AU (in preparation for Solar Probe+ and Solar Orbiter).

MESSENGER ICME Database

Winslow et al. (2015) JGR

Used observations from MESSENGER in orbit around Mercury to study ICMEs near 0.3 AU.

- Cataloged nearly 70 ICMEs at Mercury between 2011 - 2015.

- Investigated key ICME property changes from Mercury to 1 AU.

Results:

- Good agreement with previous studies for magnetic field strength dependence on distance, and evidence that ICME deceleration continues past the orbit of Mercury.

- This ICME database useful for multipoint spacecraft studies of recent ICMEs, as well as for model validation of ICME properties.

Case study: ICME in conjunction

Winslow et al. (2016) JGR

ICME from 29 December 2011 observed in "perfect" longitudinal alignment at MESSENGER and STEREO A.

From force-free field modeling, orientation of the underlying flux rope underwent a rotation of ~80◦ in latitude and ~ 65◦ in longitude between MESSENGER and STEREO A.

Based on both spacecraft observations as well as ENLIL model simulations of the steady state solar wind, we find that interaction involving magnetic reconnection with corotating structures in the solar wind dramatically alters the ICME magnetic field.

The strong influence of disturbances in the solar wind on ICMEs during propagation has significant implications for space weather forecasting and should serve as a caution on using very distant observations to predict the geoeffectiveness of large interplanetary transients.

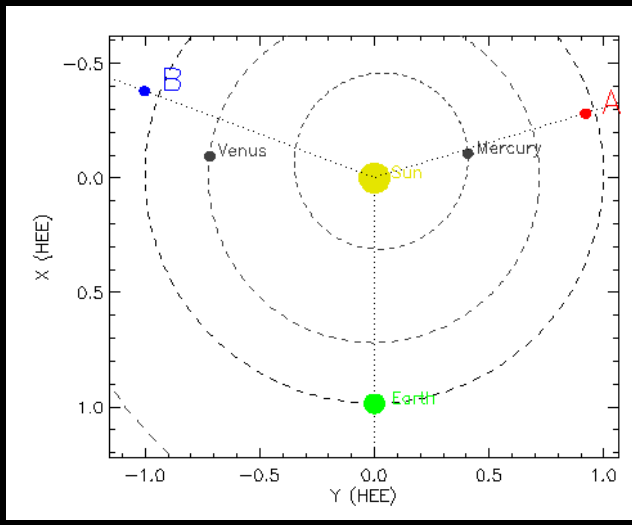

Opening a window on ICME related GCR modulation in the inner solar system

- Forbush decreases in GCR count rates indicate ICME related GCR modulation.
- We investigate changes with heliospheric distance in GCR modulation by ICMEs in the inner heliosphere using data from MESSENGER, LRO, and MSL for an ICME in conjunction.
- ICME launched on 12 Feb 2014 – Close longitudinal alignment between Mercury, Earth/Moon, and alignment within 30° with Mars. ENLIL simulation shows ICME reaching all 3 planets.

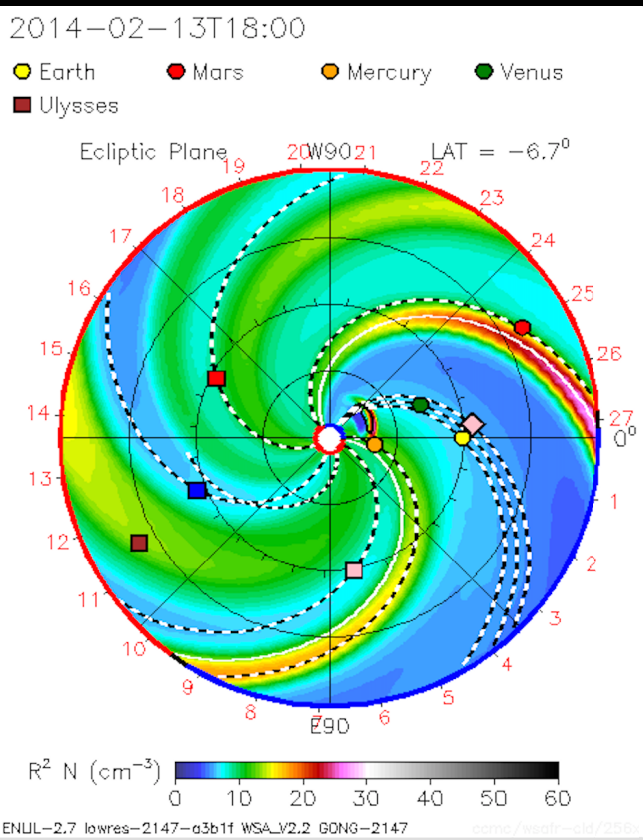

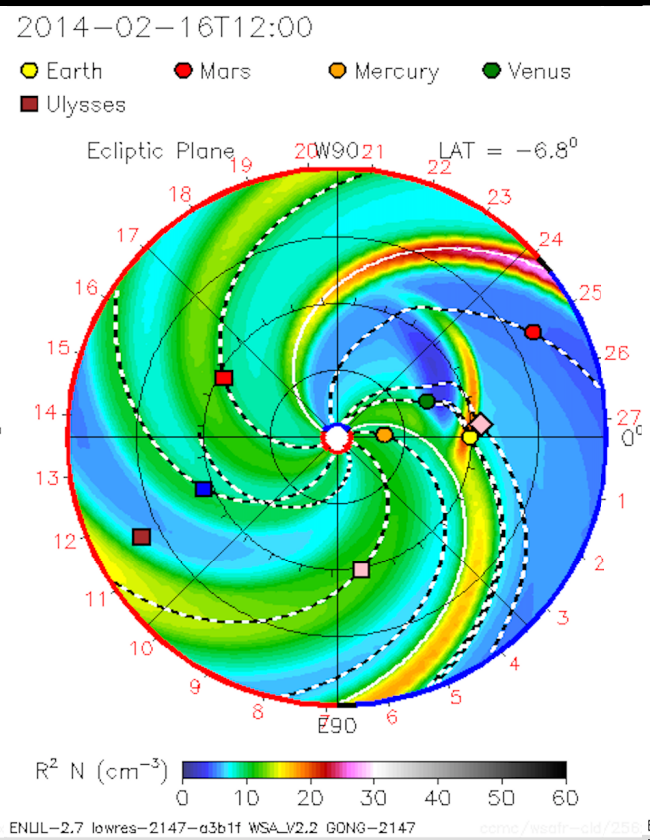

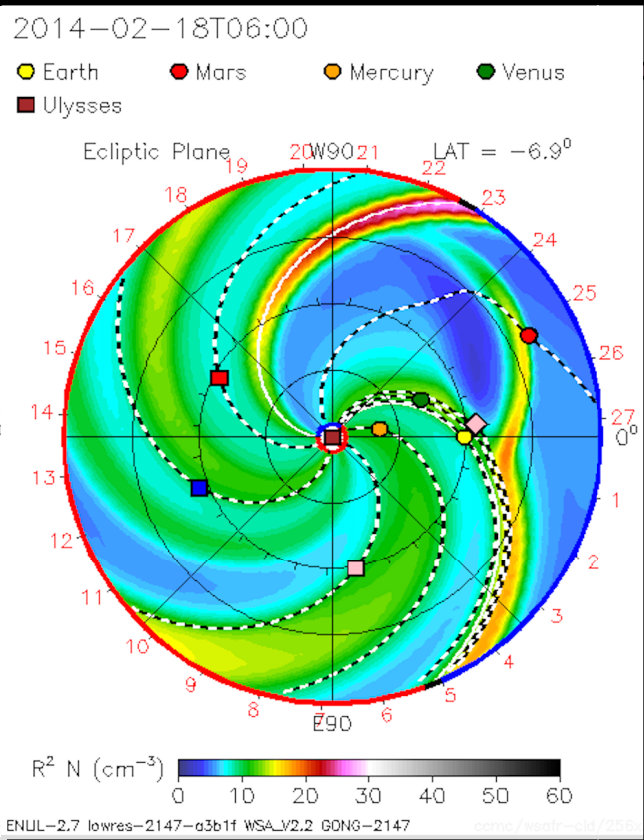

Opening a window on ICME related GCR modulation in the inner solar system

- Multipoint observations show depth of Forbush decrease diminishes with distance from Sun.
- Glimpse of environment we are about to explore with Solar Probe+, Solar Orbiter